

Iterative statistical approach to blind image deconvolution

Edmund Y. Lam and Joseph W. Goodman

Information Systems Laboratory, Department of Electrical Engineering, Stanford University, Stanford, California 94305

Received April 19, 1999; revised manuscript received October 25, 1999; accepted February 24, 2000

Image deblurring has long been modeled as a deconvolution problem. In the literature, the point-spread function (PSF) is often assumed to be known exactly. However, in practical situations such as image acquisition in cameras, we may have incomplete knowledge of the PSF. This deblurring problem is referred to as blind deconvolution. We employ a statistical point of view of the data and use a modified maximum *a posteriori* approach to identify the most probable object and blur given the observed image. To facilitate computation we use an iterative method, which is an extension of the traditional expectation-maximization method, instead of direct optimization. We derive separate formulas for the updates of the estimates in each iteration to enhance the deconvolution results, which are based on the specific nature of our *a priori* knowledge available about the object and the blur. © 2000 Optical Society of America [S0740-3232(00)00507-X]

OCIS codes: 100.1830, 100.3020, 100.2000, 000.5490, 110.5200.

1. INTRODUCTION

In many imaging situations, such as image capture with a consumer camera, the optical system can be regarded as a system with incoherent illumination. Under these circumstances, the object and the image are related in the frequency domain by

$$\mathcal{G}_i(f_x, f_y) = \mathcal{H}(f_x, f_y)\mathcal{G}_g(f_x, f_y), \quad (1)$$

where \mathcal{G}_i is the normalized frequency spectrum of the image intensity $i(x, y)$, \mathcal{G}_g is the normalized frequency spectrum of the object intensity $g(x, y)$, and \mathcal{H} is the optical transfer function.¹ Noise is inevitably present in any imaging system and is customarily modeled as additive white Gaussian noise at the output when the dominant source is the random thermal motion of electrons.² A uniform-noise assumption is also common for the quantization-noise distribution,³ while Poisson noise is typically used for astronomical images, which are taken at low light levels. Taking Eq. (1) to the space domain by inverse Fourier transforms and including the contribution of noise, we arrive at the convolution equation

$$i(x, y) = h(x, y) * g(x, y) + n(x, y), \quad (2)$$

where $h(x, y)$, called the point-spread function, is the inverse Fourier transform of $\mathcal{H}(f_x, f_y)$ and $n(x, y)$ is the additive noise. $h(x, y)$ could represent many space-invariant blurs, the most common being defocus and motion blurs. Given an image $i(x, y)$, our goal is to undo the blurring and recover as close an approximation to the object $g(x, y)$ as possible. From Eq. (2) we see that deblurring could be cast as a deconvolution problem. It is called blind image deconvolution when the blur $h(x, y)$ is not known precisely.

Successful blind deconvolution operations would have a significant impact on digital photography. In addition to facilitating easy transmission and sharing of pictures, digitized photographs allow us to take advantage of the

ever-increasing computational power available in image postprocessing in order to enhance the quality of the final output images. If blind deconvolution can be done successfully in the camera or in a postcapture workstation, we may choose to sacrifice some precision of the instruments and instead rely on the postprocessing to fine tune the images. For example, we might not require precise positioning of the lens for focusing but can correct for the error by digital restoration. This is possible when the amount of defocusing is known,⁴ but blind deconvolution would take that one step further to allow for errors in the estimated extent of the defocus. The aim of our research work is to derive blind image deconvolution algorithms that could eventually be implemented for digital photography.

This paper is organized as follows: In Section 2 we present a novel classification of the literature on blind deconvolution of images. The classification is based on three disparate notions of what is to be considered a solution, so the reader can gain an appreciation of the richness of this problem. Then in Section 3 we formulate a statistical algorithm related to the maximum *a posteriori* (MAP) technique from a Bayesian point of view, which can be considered an extension to the maximum-likelihood (ML) deconvolution.⁵ We first briefly review the method, as well as the expectation-maximization (EM) technique commonly used, before applying it to blind image deconvolution. After we have presented our algorithm, in Section 4 we test it on some blurred and noisy images. We include both synthetic and photographic blurs and also compare our method with the ML deconvolution technique.

2. CLASSIFICATION OF THE LITERATURE

The existing literature on blind deconvolution differs fundamentally on the notion of a solution, which in turn leads to different mathematical approaches to solve the

problem. Broadly speaking, they can be classified into three groups:

1. In the first group, one considers the noiseless case and uses the z -domain equivalence of Eq. (2) as the imaging equation. The deconvolution problem is then equivalent to a factorization problem of a bivariate polynomial, which is almost always unique owing to the absence of the fundamental theorem of algebra for dimensions higher than one. One then concludes that there could only be one possible object with one possible blur. Different blind deconvolution algorithms employ a variety of methods for the factorization, the most well known being the cepstrum and zero-sheet separations. The approaches have all been algebraic in nature.⁶⁻⁹

2. In the second group, it is recognized that noise is present in any imaging system and that therefore the blind deconvolution problem is inherently underdetermined with only one observation. There are, in general, a collection of possible objects and blurs that would give rise to the observed image. One seeks to impose more *a priori* constraints on the object and the blur, such as non-negativity and finite support, to reduce the set of feasible solutions. One then constructs efficient ways to find an object and a blur that satisfy all the constraints. However, any solution within the set is considered equally acceptable. Because of the difficulty in finding an object and a blur that simultaneously satisfy all the constraints, iterative solutions are usually employed.¹⁰⁻¹³

3. In the third group, one adopts a metric on the feasible solution set to identify the best solution. The rationale is that among all possible candidates for the object and the blur, some are more likely to occur than others. Each candidate is therefore associated with a probability of occurrence, and our goal is to find the object and the blur that are more likely than others, which is usually done with established statistical tools.¹⁴⁻¹⁶

All three methods have been explored with respect to their merits and applications. We employ the statistical method here for our situation of solving blind deconvolution in the context of digital photography. In particular, we will use a variant of the MAP technique, which has been used for image deconvolution with known blur.¹⁶⁻¹⁸ It has also been applied to blind deconvolution of astronomical images that are degraded by turbulence and photon noise.¹⁹ However, to solve the nonlinear optimization, it was necessary to impose severe limitations on the number of unknown parameters.²⁰ This is acceptable for astronomical images that could be modeled with only a few parameters, such as the location of the stars, but not so for digital photography, which is our focus here.

3. STATISTICAL ESTIMATION ALGORITHM

We first review the general MAP principle and the extension to the traditional EM algorithm, which is a powerful tool for solving an incomplete-data problem, before applying it to blind image deconvolution.

A. Mathematical Foundation

Let y be a realization of a stochastic process governed by a family of parameters, which we could lump together as Θ ,

and Ω_θ be the space of all the parameters. We want to find the most probable Θ given an observation of y ; i.e., we want to maximize $p(\Theta|y)$, where $p(\cdot)$ denotes the probability density function (pdf). By Bayes's rule,

$$p(\Theta|y) = \frac{p(y|\Theta)p(\Theta)}{p(y)} \\ \propto p(y|\Theta)p(\Theta), \quad (3)$$

where, since y is given, $p(y)$ is a constant and does not play any role in the maximization. Furthermore, the optimization problem is equivalent to maximizing a monotonic transformation of the terms on the right, the logarithm being commonly used. Therefore

$$\hat{\Theta} = \arg \max_{\Theta \in \Omega_\theta} p(\Theta|y). \\ = \arg \max_{\Theta \in \Omega_\theta} [\log p(y|\Theta) + \log p(\Theta)]. \quad (4)$$

This estimate is often called the maximum *a posteriori* (MAP) estimate, because we are maximizing the probability of the parameters after we have observed the output. $p(\Theta)$ contains information about our prior knowledge of the unknown parameters. If $p(\Theta)$ is considered a constant, the method becomes maximum-likelihood (ML) estimation. The incorporation of the term $p(\Theta)$ has many advantages. For image restoration, it could lead to better results because we can restore the portion of the object in the null space of the blur.¹⁶ It could also lead to faster convergence as the prior knowledge becomes more accurate. In actual implementation, often the distribution of Θ is not explicitly known. In such cases, $\log p(\Theta)$ is customarily substituted for by a penalty function quantifying the extent that Θ departs from our *a priori* knowledge.¹⁹ This will be our approach for blind deconvolution, as explained in Subsection 3.B.

Note that Eq. (4) is generally nonlinear in Θ and is difficult to evaluate for many incomplete-data problems.²¹ Although direct maximization is sometimes possible, such as using gradient-based optimization methods, it is usually convenient to employ the EM algorithm, which permits the complicated nonlinear maximization to be replaced by a computationally easier, but repeated, maximization of a related functional.²² The traditional EM algorithm is used to evaluate ML problems, but it can be extended for MAP problems.²¹ To do so, we define a new variable, z , which is called the complete data, while y is usually a part of z and is called the incomplete data. y is observable, but the missing data, i.e., the portion of z other than y , is not observable. At the beginning, we fill in the missing data by their expected values, using the observable data and the current estimate of the parameters. This is called the E step. Now with the complete data we can reestimate the unknown parameters. This process should be much easier to implement than the original problem in Eq. (4). The estimation is done by optimizing a certain functional, and this is known as the M step. With a new estimation of the unknown parameters, the missing data are no longer the expected values, so we discard them and insert new values for the missing data by using new expectations. This again induces a new opti-

mized estimation of the unknown parameters, so we need to evaluate the E step and the M step alternately.²³ When the old and the new expected values are the same, no further iteration is necessary.

For mathematical formulation of the above discussion, the extended EM algorithm has the following two equations:

$$\text{E step: } L(\Theta) = E[\log p(z; \Theta) | y; \hat{\Theta}^{(k)}], \quad (5)$$

$$\text{M step: } \hat{\Theta}^{(k+1)} = \arg \max_{\Theta \in \Omega_\theta} [L(\Theta) + \log p(\Theta)], \quad (6)$$

where the superscript indexes the number of the iteration. $L(\Theta)$ is called the conditional-likelihood function. Under fairly general conditions, this algorithm converges to a local optimum and is numerically stable.²¹ In fact, these properties can be established for a more general case, where in the M step we require $\hat{\Theta}^{(k+1)}$ only to produce a larger objective function than the previous step. There are many advantages in using the EM algorithm, including easy adaptability to estimation problems (by formulating the unknowns as the missing data) and low cost per iteration.²¹ For more discussions of the theory and applications of EM, the reader is referred to Refs. 21 and 22.

B. Blind Deconvolution with Use of the Maximum *a posteriori* Approach

Let \mathbf{g} , \mathbf{i} , and \mathbf{n} be the lexicographic ordering of the object $g(x, y)$, image $i(x, y)$, and noise $n(x, y)$ respectively. We assume the object to be of size $N \times N$, so the vectors are all of length N^2 . \mathbf{g} is adjusted to have mean equal to zero. The imaging equation can then be rewritten as a matrix equation $\mathbf{i} = H\mathbf{g} + \mathbf{n}$, where H embeds the information from $h(x, y)$.

For a linear space-invariant imaging system, H is required only to be block Toeplitz. However, in many cases it is approximated as block circulant, because the equations can then be readily converted from matrix computations to frequency-domain evaluations.²⁴ For a typical-size image, the gain in computational efficiency often far outweighs the slight compromise in quality around the edges of the images. In addition, we also assume that \mathbf{g} is a realization of a zero-mean Gaussian random process, consistent with Refs. 14 and 15. The reader should be cautioned that this is not a very accurate assumption in practice. Real images are known to possess a non-Gaussian distribution of pixel intensities; for instance, the existence of a background (such as the sky) usually skews the distribution. Rather, Gaussianity is assumed on the basis of simplicity and convenience:

- A zero-mean Gaussian distribution depends only on the covariance matrix, which is related to the power spectral density of the image by a Fourier transform.
- Linear transformation of a Gaussian distribution is also Gaussian.
- The conditional-likelihood function can be expressed analytically.

Gaussianity is critical to keeping this otherwise formidable problem more tractable. For a Gaussian distribution, the pdf of \mathbf{g} can be written explicitly as

$$p_g(\mathbf{g}) = \frac{1}{[\det(2\pi\phi_g)]^{1/2}} \exp\left(-\frac{1}{2}\mathbf{g}^T\phi_g^{-1}\mathbf{g}\right), \quad (7)$$

where we have used the symbol ϕ_g to denote the covariance matrix of \mathbf{g} .

To cast the blind image deconvolution problem in a statistical framework, our goal is to evaluate

$$\begin{aligned} \hat{\Theta} &= \arg \max_{\Theta \in \Omega_\theta} p(\Theta | \mathbf{i}) \\ &= \arg \max_{\Theta \in \Omega_\theta} [\log p(\mathbf{i} | \Theta) + \log p(\Theta)], \end{aligned} \quad (8)$$

as in Eq. (4), since \mathbf{i} is the only observable datum. For the unknown parameters we can tune, we have $\Theta = \{\phi_g, H\}$, assuming that ϕ_n is known beforehand. In fact, with an assumption of white Gaussian noise, ϕ_n is just a Kronecker delta function scaled by the variance of the noise σ_n^2 , which can be estimated by other well-known methods before we begin the blind deconvolution.

Next we have to choose an appropriate complete-data space and decide on the unknown parameters to be tuned for the optimization. Katsaggelos and Lay⁵ studied three different choices in detail and concluded that the most obvious choice, $\mathbf{z} = [\mathbf{g}^T \ \mathbf{i}^T]^T$, worked best. Note that \mathbf{i} is a zero-mean multivariate Gaussian random vector because \mathbf{g} is, and therefore \mathbf{z} is also a zero-mean multivariate Gaussian random vector. As a result, the distribution of \mathbf{z} is also dependent only on the covariance matrix, which can be related to ϕ_g and ϕ_n by

$$\begin{aligned} \phi_z &= \begin{bmatrix} \phi_g & \phi_{gi} \\ \phi_{ig} & \phi_i \end{bmatrix} \\ &= \begin{bmatrix} \phi_g & \phi_g H^T \\ H \phi_g & H \phi_g H^T + \phi_n \end{bmatrix}. \end{aligned} \quad (9)$$

The logarithm of the pdf of \mathbf{z} is written as

$$\log p_z(\mathbf{z}) = -\frac{1}{2} [\log(2\pi) + \log \det(\phi_z) + \mathbf{z}^T \phi_z^{-1} \mathbf{z}]. \quad (10)$$

From Eq. (9) we see that Θ and ϕ_n together determine ϕ_z , which in turn completely characterizes the distribution of the complete-data \mathbf{z} . Therefore Θ contains all the adjustable parameters for the optimization problem. To solve Eq. (8) by the EM algorithm, we need

$$\text{E step: } L(\Theta) = E[\log p(\mathbf{z}; \Theta) | \mathbf{i}; \hat{\Theta}^{(k)}], \quad (11)$$

$$\text{M step: } \hat{\Theta}^{(k+1)} = \arg \max_{\Theta \in \Omega_\theta} [L(\Theta) + \log p(\Theta)]. \quad (12)$$

E step: We want to evaluate $E[\log p_z(\mathbf{z}) | \mathbf{i}; \hat{\Theta}^{(k)}]$. For simplicity in notation, $\hat{\Theta}^{(k)}$ is suppressed; i.e., when an expression is conditioned on \mathbf{i} , it is understood to be conditioned on both \mathbf{i} and $\hat{\Theta}^{(k)}$. Note from Eq. (9) that ϕ_z is

independent of \mathbf{i} and $\hat{\Theta}^{(k)}$. Using the identity that $\mathbf{z}^T \phi_z^{-1} \mathbf{z} = \mathbf{g}^T \phi_g^{-1} \mathbf{g} + \mathbf{n}^T \phi_n^{-1} \mathbf{n}$ as provided in Appendix A, we have

$$E[\log p_z(\mathbf{z})|\mathbf{i}] = -\frac{1}{2}\{\log(2\pi) + \log \det(\phi_z)\} \\ + E[\mathbf{g}^T \phi_g^{-1} \mathbf{g}|\mathbf{i}] + E[\mathbf{n}^T \phi_n^{-1} \mathbf{n}|\mathbf{i}]. \quad (13)$$

The terms on the right-hand side of Eq. (13) can be analyzed as follows:

- $\log(2\pi)$ is a constant.
- From expression (9), one can easily derive that $\log \det(\phi_z) = \log \det(\phi_g) + \log \det(\phi_n)$ (see Appendix A). Using the block-circulant assumption on the matrices, we can evaluate this in the frequency domain as⁵

$$\log \det(\phi_z) = \sum_{f_x} \sum_{f_y} \log \Phi_g(f_x, f_y) + \sum_{f_x} \sum_{f_y} \log \Phi_n(f_x, f_y), \quad (14)$$

where Φ_g is the power spectrum of the object and is equal to the Fourier transform of ϕ_g . The indices trace through the entire image.

- We first rewrite $E[\mathbf{g}^T \phi_g^{-1} \mathbf{g}|\mathbf{i}]$ as $\text{Tr}\{\phi_g^{-1} E[\mathbf{g}\mathbf{g}^T|\mathbf{i}]\}$, where Tr denotes the trace operator. This is further expanded as

$$\text{Tr}\{\phi_g^{-1} E[\mathbf{g}\mathbf{g}^T|\mathbf{i}]\} = \text{Tr}\{\phi_g^{-1} \phi_{g|i}\} \\ + \text{Tr}\{\phi_g^{-1} (E[\mathbf{g}|\mathbf{i}]E[\mathbf{g}|\mathbf{i}]^T)\}. \quad (15)$$

It is important to realize that $E[\mathbf{g}|\mathbf{i}] \neq 0$, but in the frequency domain, its equivalent is the celebrated Wiener filter estimate, i.e.,

$$W_{g|i}^{(k)}(f_x, f_y) = \frac{\mathcal{H}^{*(k)}(f_x, f_y)}{|\mathcal{H}^{(k)}(f_x, f_y)|^2 + \frac{\Phi_n(f_x, f_y)}{\Phi_g^{(k)}(f_x, f_y)}} \mathcal{G}_i(f_x, f_y). \quad (16)$$

This frequency-domain evaluation is consistent with the block-circulant assumption on the blur operation. A more detailed derivation of Eq. (16) from the matrices can be found in Ref. 25. Note that $\text{Tr}\{E[\mathbf{g}|\mathbf{i}]E[\mathbf{g}|\mathbf{i}]^T\} = (1/N^2) \sum_{f_x} \sum_{f_y} |W_{g|i}^{(k)}(f_x, f_y)|^2$ by Parseval's theorem. As for the variance, after some derivation (see Appendix A) we arrive at the frequency-domain expression

$$\Phi_{g|i}^{(k)}(f_x, f_y) = \frac{\Phi_g^{(k)}(f_x, f_y)}{\Phi_i^{(k)}(f_x, f_y)} \Phi_n(f_x, f_y). \quad (17)$$

So the whole expression can be written as

$$E[\mathbf{g}^T \phi_g^{-1} \mathbf{g}|\mathbf{i}] \\ = \sum_{f_x} \sum_{f_y} \frac{\Phi_{g|i}^{(k)}(f_x, f_y) + (1/N^2) |W_{g|i}^{(k)}(f_x, f_y)|^2}{\Phi_g(f_x, f_y)}. \quad (18)$$

- Since we assumed that ϕ_n is known, $\mathbf{n}^T \phi_n^{-1} \mathbf{n}$ is a constant.

Therefore, if we use the symbol K to represent all the constant terms, expression (13) can be simplified as

$$L(\Theta) = K - \frac{1}{2} \sum_{f_x} \sum_{f_y} \left[\log \Phi_g(f_x, f_y) \right. \\ \left. + \frac{\Phi_{g|i}^{(k)}(f_x, f_y) + (1/N^2) |W_{g|i}^{(k)}(f_x, f_y)|^2}{\Phi_g(f_x, f_y)} \right]. \quad (19)$$

M step: A MAP formulation stipulates an extra regularization term, $\log p(\Theta) = \log p(\phi_g) + \log p(H)$, to be added to expression (19) for maximization. Note that we are regularizing ϕ_g and H because they are the parameters that we can tune. We know *a priori* that ϕ_g should be smooth. Since this is usually not expressed explicitly as a probability distribution of $p(\phi_g)$, we propose two methods that work well in practice:

1. We add a penalty term for the roughness, or irregularity, of ϕ_g in expression (19), which manifests itself as a high-pass filtering of Φ_g . Let the high-pass filter be V , such as the Laplacian or the Laplacian of Gaussian operators,² and let the amount of regularization be controlled by a parameter α , which depends on the nature of the images. It can be chosen by many different schemes.¹¹ The nonconstant terms of Eq. (19) together with the regularization terms can now be expressed as

$$\tilde{L}(\Theta) = \sum_{f_x} \sum_{f_y} \left[\log \Phi_g(f_x, f_y) \right. \\ \left. + \frac{\Phi_{g|i}^{(k)}(f_x, f_y) + (1/N^2) |W_{g|i}^{(k)}(f_x, f_y)|^2}{\Phi_g(f_x, f_y)} \right. \\ \left. + \alpha V(f_x, f_y) \Phi_g(f_x, f_y) \right]. \quad (20)$$

Setting $\partial L / \partial \Phi_g = 0$, we have, after some simplifications,

$$\Phi_g^{(k+1)}(f_x, f_y) = \frac{-1 + \{1 + 4\alpha V(f_x, f_y) [\Phi_{g|i}^{(k)}(f_x, f_y) + (1/N^2) |W_{g|i}^{(k)}(f_x, f_y)|^2]\}^{1/2}}{2\alpha V(f_x, f_y)}. \quad (21)$$

As $\alpha \rightarrow 0$, using $(1 + \alpha x)^{1/2} \approx 1 + \alpha x/2$, we have

$$\Phi_g^{(k+1)}(f_x, f_y) = \frac{-1 + 1 + \frac{1}{2} \{4\alpha V(f_x, f_y) [\Phi_{g|i}^{(k)}(f_x, f_y) + (1/N^2) |W_{g|i}^{(k)}(f_x, f_y)|^2]\}}{2\alpha V(f_x, f_y)} \\ = \Phi_{g|i}^{(k)}(f_x, f_y) + \frac{1}{N^2} |W_{g|i}^{(k)}(f_x, f_y)|^2, \quad (22)$$

which would be the updated equation for unregularized restoration.

2. When speed or memory storage is a concern, such as when we are performing restoration within a camera, we could set $\Phi_g^{(k)}$ to be an unknown constant, implying that we assume the signal is white. This is an extension of pseudoinverse filtering in ordinary image restoration.² In that case, instead of using the regularized equation [Eq. (21)], we need only take the mean of the estimation from Eq. (22), i.e.,

$$\begin{aligned} \Phi_g^{(k+1)}(f_x, f_y) &= \frac{1}{N^2} \sum_{f_x} \sum_{f_y} \left[\Phi_{g|i}^{(k)}(f_x, f_y) + \frac{1}{N^2} |W_{g|i}^{(k)}(f_x, f_y)|^2 \right]. \end{aligned} \quad (23)$$

Our next step is to update \mathcal{H} . From the imaging equation [Eq. (1)], we know that \mathcal{H} is the ratio of the observed image to the estimated object, i.e.,

$$\mathcal{H}(f_x, f_y) \approx \frac{G_i(f_x, f_y)}{W_{g|i}(f_x, f_y)} \approx \frac{1}{N^2} \frac{G_i(f_x, f_y) W_{g|i}^*(f_x, f_y)}{\Phi_g(f_x, f_y)}. \quad (24)$$

The second expression is preferred because we have also made use of Φ_g , which incorporates our *a priori* knowledge of the image spectrum. To impose *a priori* constraints on \mathcal{H} needs a different strategy. Again, the knowledge about \mathcal{H} is seldom given in the form of a pdf. Rather, we usually know that the blur that we have belongs to a subset of all possible blurs. For instance, \mathcal{H} usually possesses some symmetry,¹ and we may even

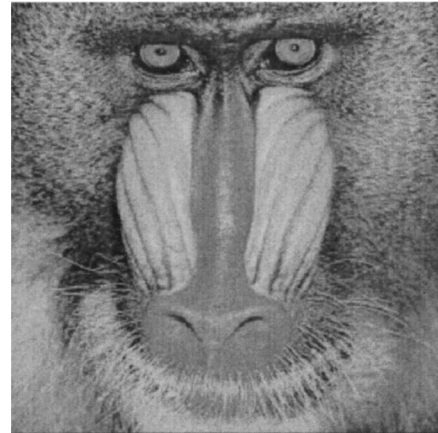


Fig. 1. "Baboon" test image.

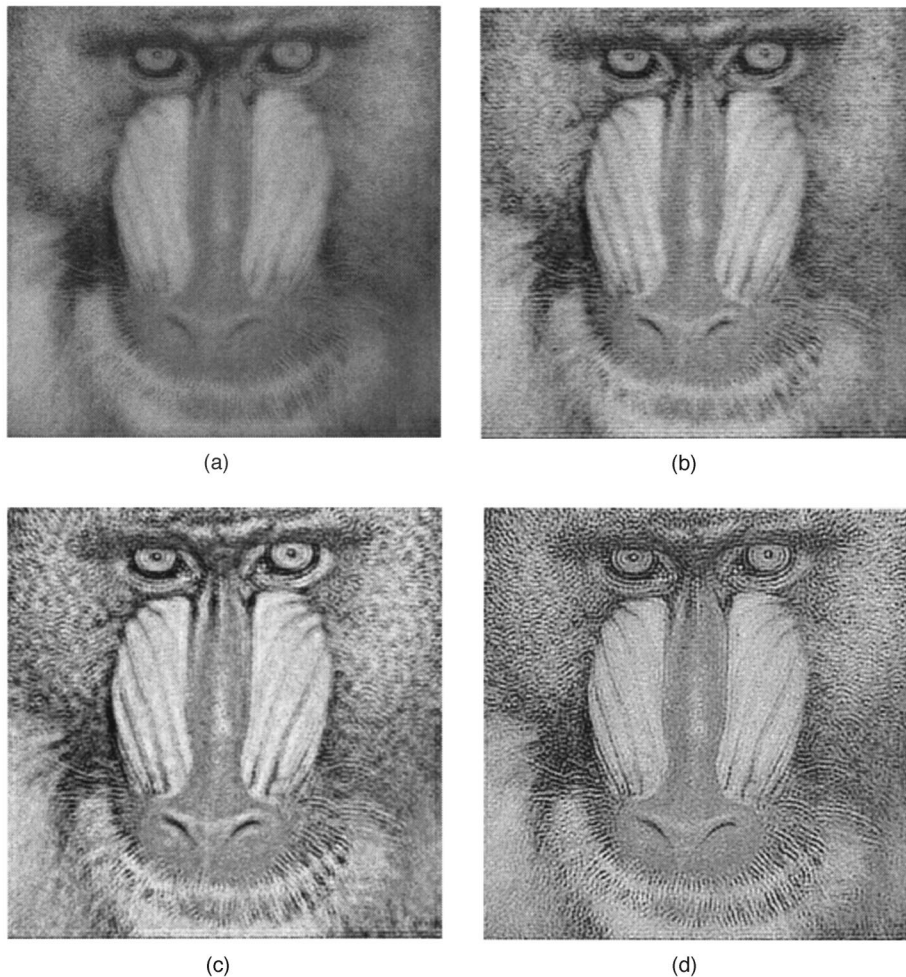


Fig. 2. Simulated image restoration: (a) blurred image, (b) image restored by our first method, (c) image restored by our second method, (d) image restored by the ML method.

know the nature of the blur (e.g., defocus). We represent such knowledge with a set \mathcal{C}_H , which contains all candidates for possible blurs. This set is convex for nonnegativity, finite support constraints, and defocus blurs and is also convex for motion blur if the direction of blur is estimated beforehand. Therefore the best estimate for \mathcal{H} is found by the following optimization problem:

$$\begin{aligned} &\text{minimize} && \sum_{f_x} \sum_{f_y} \left[\mathcal{H}(f_x, f_y) \right. \\ &&& \left. - \frac{\mathcal{G}_i(f_x, f_y) W_{gi}^{*(k)}(f_x, f_y)}{N^2 \Phi_g^{(k+1)}(f_x, f_y)} \right]^2 \\ &\text{subject to} && \mathcal{H} \in \mathcal{C}_H. \end{aligned} \tag{25}$$

Depending on the amount of *a priori* knowledge, we may not have an analytic expression for \mathcal{H} ; however, since it is a convex optimization problem, fast algorithms exist for the computation to yield $\mathcal{H}^{(k+1)}(f_x, f_y)$. Finally, note that in each iteration the restored image is given by the inverse Fourier transform of the Wiener filter estimate from Eq. (16).

4. SIMULATIONS

For artificial blurring we take the image “baboon” shown in Fig. 1 from the standard image-processing library for simulation. The size of the image is 256×256 . This image is subjected to a space-invariant out-of-focus blur, with the severity parameter $W_m/\lambda = 0.5$.^{1,4} White Gaussian noise is then added to the blurred image. The noise amount is specified by the signal-to-noise ratio (SNR), which is defined as²⁶

$$\text{SNR}(g, n) = 10 \log_{10} \left\{ \frac{\sum_x \sum_y [g(x, y)]^2}{\sum_x \sum_y [n(x, y)]^2} \right\}, \tag{26}$$

where n is the amount of noise added. In Fig. 2(a), we show the blurred and noisy image with an SNR equal to 30 dB. Figure 2(b) shows the restored image after five iterations, where we used Eq. (21) as our regularization. In the simulation we use a high-pass filter V , which is the Fourier transform of the 3×3 Laplacian kernel

$$v = \begin{bmatrix} -1 & -1 & -1 \\ -1 & 8 & -1 \\ -1 & -1 & -1 \end{bmatrix}. \tag{27}$$

The regularization parameter α is chosen by the Miller bound method.²⁷ We constrain \mathcal{H} to be circularly symmetric with nonnegative values and with frequency content below the in-focus optical transfer function, since aberration in general cannot increase contrast of images.¹ We can see that the visual quality has improved significantly. Running the algorithm for more iterations produces negligible change in the visual appearance, indicating that the restoration has likely stabilized. In Fig. 2(c) we change to using Eq. (23) as our regularization equation, and the restored image quality is still acceptable.

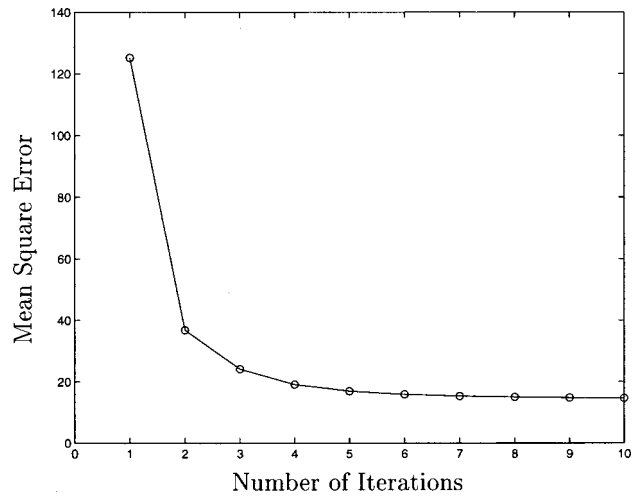
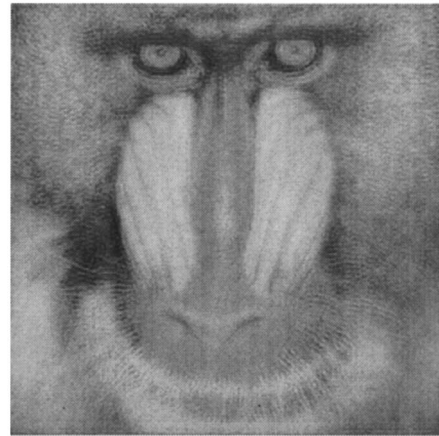
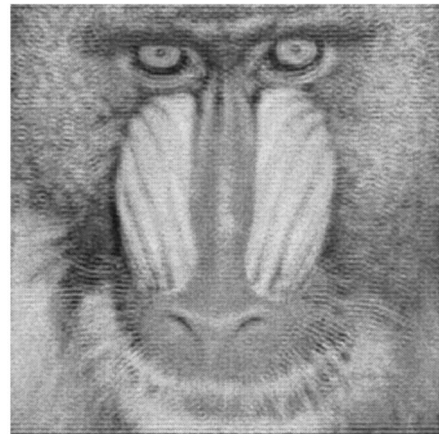


Fig. 3. Blur estimation error.



(a)



(b)

Fig. 4. Simulated image restoration for uniform noise: (a) blurred image, (b) image restored by our first method.

In Fig. 2(d) the image from (a) is subjected to the ML restoration method from Ref. 5. The restored image appears to have an irregular spectrum, consistent with some sample images shown in that paper.

Although it is hard to quantify the improvement in the restored image quality because the metric needs to corre-

spond to the human visual system, we can measure the improvement in blur identification more easily by using simply the l_2 norm. Figure 3 shows the error of the blur estimation compared with the blur used in the simulation as a function of the number of iterations. We can see that the estimation error decreases with time and approaches a constant after less than ten iterations. This shows that the blur does not change much after a few iterations. The change in the blur estimation could therefore be used as a termination criterion for the restoration.

Next we change the noise to uniform noise with the same SNR for the case where quantization noise is dominant. Figure 4(a) shows the noisy and blurred baboon image, and Fig. 4(b) shows the restored image, again with only five iterations. It appears that, although the algorithm is derived for Gaussian noise (with the use of Wiener filters), it can be applicable for uniform noise as well.

Finally, we tested the algorithm on a photographic blurred image as shown in Fig. 5(a). This is a picture of the Chicago Navy Pier taken from a boat. The object is clearly out of focus and possibly suffers from motion blur as well because of the rocking of the waves. Therefore we relax the constraints on \mathcal{H} so that it can accommodate for the motion blur, while noticing the fact that the dominant

aberration is defocus. This is achieved by taking a linear combination of the estimate of \mathcal{H} given the stronger constraints, as done previously, and when \mathcal{H} is unconstrained. Figure 5(b) shows the image after five iterations of the algorithm. The restored image looks sharper, and we can now see the patterns better on the two towers.

5. CONCLUSIONS

In this paper we extended the maximum-likelihood (ML) blind deconvolution method treated in the literature by incorporating prior knowledge about the blur and the object. Since the nature of the *a priori* information for the blur and for the object power spectrum are usually different, we used regularization and constrained optimization for the updates of the object spectrum and blur function respectively. Experimental results confirmed the versatility and the power of our method. We also have a method for updates in the iteration that is simpler than the ML method, representing progress toward our eventual goal of applying blind deconvolution to programmable digital cameras.

APPENDIX A

In this paper we claimed that for $\mathbf{i} = H\mathbf{g} + \mathbf{n}$ and $\mathbf{z} = [\mathbf{g}^T \ \mathbf{i}^T]^T$, we have $\mathbf{z}^T \phi_z^{-1} \mathbf{z} = \mathbf{g}^T \phi_g^{-1} \mathbf{g} + \mathbf{n}^T \phi_n^{-1} \mathbf{n}$. To prove that this is the case, we note that from Eq. (9), ϕ_z^{-1} is given by^{5,28}

$$\phi_z^{-1} = \begin{bmatrix} \phi_g^{-1} + H^T \phi_n^{-1} H & -H^T \phi_n^{-1} \\ -\phi_n^{-1} H & \phi_n^{-1} \end{bmatrix}. \quad (28)$$

Therefore

$$\begin{aligned} \mathbf{z}^T \phi_z^{-1} \mathbf{z} &= [\mathbf{g}^T \ \mathbf{i}^T] \begin{bmatrix} \phi_g^{-1} + H^T \phi_n^{-1} H & -H^T \phi_n^{-1} \\ -\phi_n^{-1} H & \phi_n^{-1} \end{bmatrix} \begin{bmatrix} \mathbf{g} \\ \mathbf{i} \end{bmatrix} \\ &= \mathbf{g}^T (\phi_g^{-1} + H^T \phi_n^{-1} H) \mathbf{g} + \mathbf{g}^T (-H^T \phi_n^{-1}) \mathbf{i} \\ &\quad + \mathbf{i}^T (-\phi_n^{-1} H) \mathbf{g} + \mathbf{i}^T \phi_n^{-1} \mathbf{i} \\ &= \mathbf{g}^T \phi_g^{-1} \mathbf{g} + (\mathbf{i}^T - \mathbf{n}^T) \phi_n^{-1} (\mathbf{i} - \mathbf{n}) \\ &\quad - (\mathbf{i}^T - \mathbf{n}^T) \phi_n^{-1} \mathbf{i} - \mathbf{i}^T \phi_n^{-1} (\mathbf{i} - \mathbf{n}) + \mathbf{i}^T \phi_n^{-1} \mathbf{i} \\ &= \mathbf{g}^T \phi_g^{-1} \mathbf{g} + \mathbf{n}^T \phi_n^{-1} \mathbf{n}. \end{aligned} \quad (29)$$

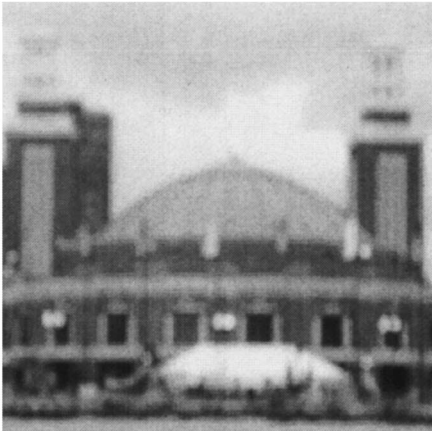
To show that $\log \det(\phi_z) = \log \det(\phi_g) + \log \det(\phi_n)$, we substitute Eq. (9) for ϕ_z to get

$$\begin{aligned} \log \det(\phi_z) &= \log \det(H \phi_g \phi_g H^T + \phi_g \phi_n - H \phi_g \phi_g H^T) \\ &= \log \det(\phi_g \phi_n) \\ &= \log \det(\phi_g) + \log \det(\phi_n). \end{aligned} \quad (30)$$

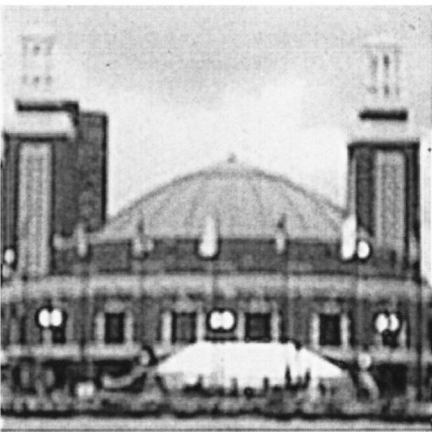
To derive the expression for Eq. (17), we first note that

$$\begin{aligned} \phi_{g|i} &= \phi_g - \phi_{gi} \phi_i^{-1} \phi_{ig} \\ &= \phi_g - \phi_g H \phi_i^{-1} H \phi_g. \end{aligned} \quad (31)$$

Therefore, in the frequency domain,



(a)



(b)

Fig. 5. Image restoration for real images: (a) blurred image, (b) image restored by our first method.

$$\begin{aligned}
& \Phi_{g|i}^{(k)}(f_x, f_y) \\
&= \Phi_g^{(k)}(f_x, f_y) - \frac{|\mathcal{H}^{(k)}(f_x, f_y)|^2 \Phi_g^{(k)}(f_x, f_y)}{\Phi_i^{(k)}(f_x, f_y)} \Phi_g^{(k)}(f_x, f_y) \\
&= \left[\frac{\Phi_i^{(k)}(f_x, f_y) - |\mathcal{H}^{(k)}(f_x, f_y)|^2 \Phi_g^{(k)}(f_x, f_y)}{\Phi_i^{(k)}(f_x, f_y)} \right] \\
&\quad \times \Phi_g^{(k)}(f_x, f_y) \\
&= \frac{\Phi_g^{(k)}(f_x, f_y)}{\Phi_i^{(k)}(f_x, f_y)} \Phi_n(f_x, f_y). \tag{32}
\end{aligned}$$

ACKNOWLEDGMENTS

This work is partially supported under the Stanford Programmable Digital Camera project by Intel, Hewlett-Packard, Kodak, Canon, and Interval Research.

REFERENCES

1. J. W. Goodman, *Introduction to Fourier Optics*, 2nd ed. (McGraw-Hill, New York, 1996).
2. K. R. Castleman, *Digital Image Processing* (Prentice-Hall, Englewood Cliffs, N.J., 1996).
3. A. Gersho and R. Gray, *Vector Quantization and Signal Compression* (Kluwer Academic, Boston, Mass., 1992).
4. E. Y. Lam and J. W. Goodman, "Discrete cosine transform domain restoration of defocused images," *Appl. Opt.* **37**, 6213–6218 (1998).
5. A. K. Katsaggelos and K.-T. Lay, "Maximum likelihood identification and restoration of images using the expectation-maximization algorithm," in *Digital Image Restoration*, A. K. Katsaggelos, ed. (Springer-Verlag, New York, 1991), pp. 143–176.
6. M. Cannon, "Blind deconvolution of spatially invariant image blurs with phase," *IEEE Trans. Acoust., Speech, Signal Process.* **24**, 58–63 (1976).
7. R. Bates, B. Quek, and C. Parker, "Some implications of zero sheets for blind deconvolution and phase retrieval," *J. Opt. Soc. Am. A* **7**, 468–479 (1990).
8. D. Ghiglia, L. Romero, and G. Mastin, "Systematic approach to two-dimensional blind deconvolution by zero-sheet separation," *J. Opt. Soc. Am. A* **10**, 1024–1036 (1993).
9. E. Y. Lam and J. W. Goodman, "Blind image deconvolution for symmetric blurs by polynomial factorization," in *18th Congress of the International Commission for Optics: Optics for the Next Millennium*, A. J. Glass, J. W. Goodman, M. Chang, A. H. Guenther, and T. Asakura, eds., *Proc. SPIE* **3749**, 174–175 (1999).
10. G. Ayers and J. Dainty, "Iterative blind deconvolution method and its applications," *Opt. Lett.* **13**, 547–549 (1988).
11. Y.-L. You and M. Kaveh, "A regularization approach to joint blur identification and image restoration," *IEEE Trans. Image Process.* **5**, 416–428 (1996).
12. D. Kundur and D. Hatzinakos, "A novel blind deconvolution scheme for image restoration using recursive filtering," *IEEE Trans. Signal Process.* **46**, 375–390 (1998).
13. E. Y. Lam and J. W. Goodman, "Iterative blind image deconvolution in space and frequency domains," in *Sensors, Cameras, and Applications for Digital Photography*, N. Sampat and T. Yeh, eds., *Proc. SPIE* **3650**, 70–77 (1999).
14. R. L. Lagendijk, A. M. Tekalp, and J. Biemond, "Maximum likelihood image and blur identification: a unifying approach," *Opt. Eng.* **29**, 422–435 (1990).
15. K.-T. Lay and A. K. Katsaggelos, "Image identification and restoration based on the expectation-maximization algorithm," *Opt. Eng.* **29**, 436–446 (1990).
16. T. J. Hebert and K. Lu, "Expectation-maximization algorithms, null spaces, and MAP image restoration," *IEEE Trans. Image Process.* **4**, 1084–1095 (1995).
17. C. Bouman and K. Sauer, "A generalized Gaussian image model for edge-preserving MAP estimation," *IEEE Trans. Image Process.* **2**, 296–310 (1993).
18. S. Z. Li, "MAP image restoration and segmentation by constrained optimization," *IEEE Trans. Image Process.* **7**, 1730–1735 (1998).
19. L. Mugnier, J.-M. Conan, T. Fusco, and V. Michau, "Joint maximum a posteriori estimation of object and PSF for turbulence degraded images," in *Bayesian Inference for Inverse Problems*, A. Mohammad-Djafari, ed., *Proc. SPIE* **3459**, 50–61 (1998).
20. J. Markham and J.-A. Conchello, "Parametric blind deconvolution: a robust method for the simultaneous estimation of image and blur," *J. Opt. Soc. Am. A* **16**, 2377–2391 (1999).
21. G. J. McLachlan and T. Krishnan, *The EM Algorithm and Extensions* (Wiley, New York, 1997).
22. A. Dempster, N. Laird, and D. Rubin, "Maximum likelihood from incomplete data," *J. R. Statist. Soc. Ser. B* **39**, 1–38 (1977).
23. R. J. Little and D. B. Rubin, *Statistical Analysis with Missing Data* (Wiley, New York, 1987).
24. H. Andrews and B. Hunt, *Digital Image Restoration* (Prentice-Hall, Englewood Cliffs, N.J., 1977).
25. A. Katsaggelos, *Digital Image Restoration* (Springer-Verlag, New York, 1991).
26. A. K. Jain, *Fundamentals of Digital Image Processing* (Prentice-Hall, Englewood Cliffs, N.J., 1989).
27. K. Miller, "Least-squares methods for ill-posed problems with a prescribed bound," *SIAM J. Math. Anal.* **1**, 52–74 (1970).
28. T. Kailath, *Linear Systems* (Prentice-Hall, Englewood Cliffs, N.J., 1980).